WOODCOATINGS

Developments for a Sustainable Future

Development of Test Apparatus for Service Life Prediction of Sealant Formulations and Evaluation of Data from 18 Months of Outdoor Weathering

Authors: Dr R. Sam Williams[1]
Steve Lacher[1]
Corey Halpin[1]
Christopher White[2]

Presented by: Dr R. Sam Williams
Supervisory Research Chemist

Company: [1] U.S. Department of Agriculture, Forest Service, Forest Products Lab.
One Gifford Pinchot Drive
Madison, Wisconsin 53726-2398
USA

[2] National Institute of Standards and Technology, USA

Tel: +1 608 231 9412

Fax: +1 608 231 9262

e-mail: rswilliams@fs.fed.us

Paper 16

A sealant test that combines cyclic stress (fatigue), water immersion, and temperature change was initially developed by A. Hockman at NIST (ASTM 2000, C 719 93) (the so-called Hockman cycle). Specimens are rated visually for cohesive or adhesive failure. Studies on the correlation of long-term artificial aging and outdoor exposure of sealants that focused on the degradation of cohesive properties and surface appearance were reviewed by Wolf (1999).

Several devices have been used to induce cyclic movement (fatigue) of sealants during exposure. These devices generally use thermally induced dimensional change to generate fatigue in a sealant. For example, Onuoha (1 999) used unplasticized polyvinyl chloride (PVC) pipe to produce fatigue in one-part polyurethane and polyurethane-hybrid sealants. Racks have also been built using dissimilar materials such as wood and aluminum (Brown 1965), concrete and aluminum (Burstrom 1980), and steel and aluminum (Karpati *et al.* 1977) to develop fatigue stresses. Manually operated devices have also been used to create cycling effects (Lacasse 1994).

In reviewing the work done in our laboratory and similar work reported by others who have developed accelerated test methods, two problems became obvious. First, weather is not consistent from day to day, season to season, year to year, and century to century (Martin 2000). Second, weather data have not been used in any meaningful way during outdoor exposure. That is, there has been no link between specific weather events and response of materials to these events. Thus, a variety of weathering events that may have had a dramatic influence on degradation were averaged out. There was no way of knowing what the conditions were when the specimens degraded. The specimens may have degraded more or less at the same rate since the previous evaluation, or all the degradation could have occurred during a single weather event, like a hailstorm. Periodic evaluations give only the change since the previous evaluation, not the conditions that caused the change. Accelerated tests were usually evaluated in the same way – periodically during the exposure. Results were often misleading because critical factors causing the degradation were either not known or not measured.

Our approach to these problems has been to develop instruments and evaluation methods that can be used in both accelerated laboratory tests and outdoor exposure tests. The materials response and the conditions in the laboratory test can then be compared with the weather data and the materials response obtained from the outdoor exposure. The FPL field site, which is 5 km west of Madison, Wisconsin, has been fully instrumented to collect weather data during outdoor exposure. This includes temperature, relative humidity (RH), precipitation, and UV radiation. The test apparatus employed have been custom built and use the movement of wood to fatigue specimens. We previously reported the materials response of two different sealant compounds during approximately 2 months of weathering (Williams *et al.* 2002). The data from outdoor tests is being merged with accelerated tests to develop reliability-based protocols for service life prediction (White *et al.* 2002) and to characterize the physical and chemical changes in sealants as they weather (Hunston *et al.* 2003a, b; White *et al.* 2003). Test apparatus have also been developed for accelerated weathering of sealants under laboratory conditions (White *et al.* 2004).

The focus of this report is to describe the results from seven different sealant formulations exposed for up to 18 months. The methods used to evaluate the data are described, the difficulties encountered in analyzing the data are discussed, and new developments in the test apparatus are presented.

Experimental

Weather Station

The weather station has a modular design, which permits flexibility in terms of the type of sensors that can be used and the ability to modify the system to meet future needs. The present configuration consists of a wind meter, a tipping bucket rain gauge, and a weather station attached to a data logger. The wind meter measures wind speed and direction. The rain gauge measures both rainfall and snowfall, using a built-in heating coil to melt snow. The weather station provides measurements of temperature, barometric pressure, and RH with extremely high accuracy. Data are stored locally in a tab-delimited database as hourly averages; however, 1-min data are extracted for calculations. Ultraviolet radiation is measured and recorded at the following wavelengths (in nanometers): 289.94, 291.30, 293.70, 295.93, 297.68, 299.70, 301.14, 303.75, 305.66, 307.47, 309.71, 312.22, 314.14, 315.76, 318.24, 319.96, 321.93, and 323.45. The UV radiometer and data collection protocol was described previously (Williams *et al.* 2002, 2004).

Test Apparatus

Three types of test apparatus have been designed and built. Two of these apparatus depend on the moisture-induced dimensional change in wood to produce cyclic fatigue. The third apparatus can use any material to produce a cyclic motion. The signal from this motion is fed to a computer that drives the cyclic fatigue. All three apparatus subject specimens to cyclic fatigue in response to weather changes.

Wood-driven apparatus

For the wood-driven apparatus, weather-induced cyclic fatigue of sealant specimens is obtained from the dimensional change in tangential blocks of red oak *(Quercus rubra)* as the wood wets and dries, from precipitation and/or changes in RH. Because the movement of the wood causes the cyclic fatigue of the specimens, it is referred to as the wood engine.

The wood moves against a rigid aluminum frame to produce a cyclic movement. The aluminum is attached to the bar at the top of the apparatus; the load cell and specimen are uniaxial and are connected using a stainless steel threaded rod with locking nuts (Fig. 1). All fasteners in the apparatus are stainless steel. Each specimen can be attached to a linear variable differential transformer (LVDT). However, we found that deflection could be determined using only four LVDTs. The apparatus is capable of giving a maximum deflection of about ±3 mm. By adjusting the size of the wood and the aluminum, the maximum movement can be controlled. The LVDTs are sealed sensors, with a deflection range of ±6.35 mm. Force transducers (load cells) are used to measure the load in the system. The sealed transducers have a capacity of ±1111 N. Specimens were instrumented to continuously monitor force and deflection. The force and deflection were then used to calculate and record the stress and strain on each of the specimens.

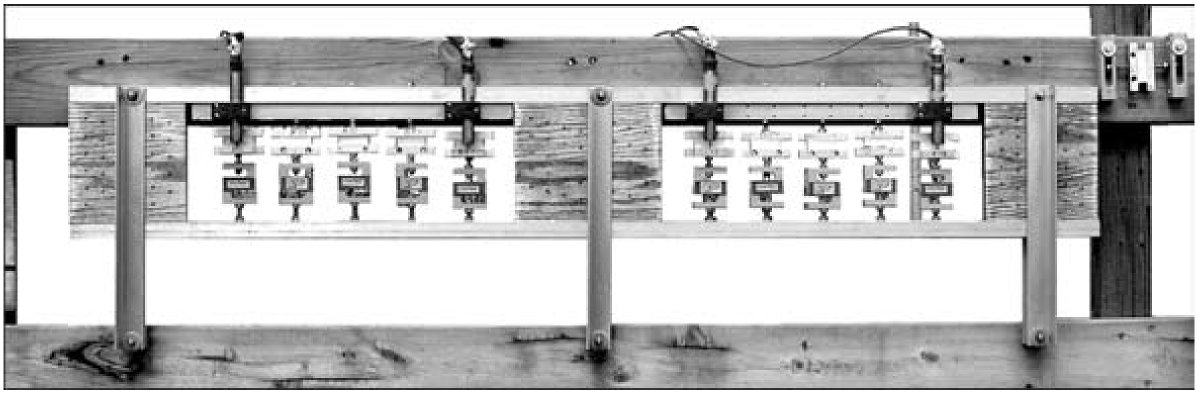

Figure 1. The CS type outdoor exposure apparatus.

Two designs (tension swell (TS) and compression swell (CS)) were developed for conducting these exposure tests. In TS (Fig. 2), the test specimens are placed in tension by an increase in moisture content of the wood (as the wood swells). This apparatus simulates the thermally driven designs previously used (Brown 1965, Karpati *et al.* 1977, Burstrom 1980, Onuoha 1999), but it is driven primarily by changes in RH and water, not temperature. In CS (Fig. 3), the test specimens are placed in compression as the wood swells, which subjects the specimens to stresses similar to that obtained when sealants are used on wood.

Computer-controlled apparatus

The requirements for the computer-controlled cyclic fatigue test apparatus (CFTA) were as follows:

1. The motors must be powerful enough to drive 10 to 20 specimens on one CFTA.
2. The apparatus must be rigid enough to ensure near equal strain on all specimens.
3. CFTA must be reliable when exposed to the weather.
4. CFTA must accurately impose strain on the specimens.
5. CFTA must be free of accumulated error.
6. CFTA design must facilitate installing and removing specimens.
7. Cost must be minimized. This demanded using as much off-the-shelf hardware as possible.

A two-beam parallel design was selected. In this design, the CFTA consists of two horizontal beams, one above the other, connected by linear actuators at each end (Fig. 4). The upper beam is fixed and the lower beam is driven up or down by the linear actuators. Specimens are placed between the beams parallel to the linear actuators.

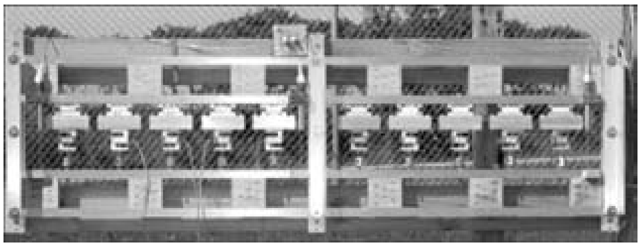

Figure 2. The TS type outdoor exposure apparatus.

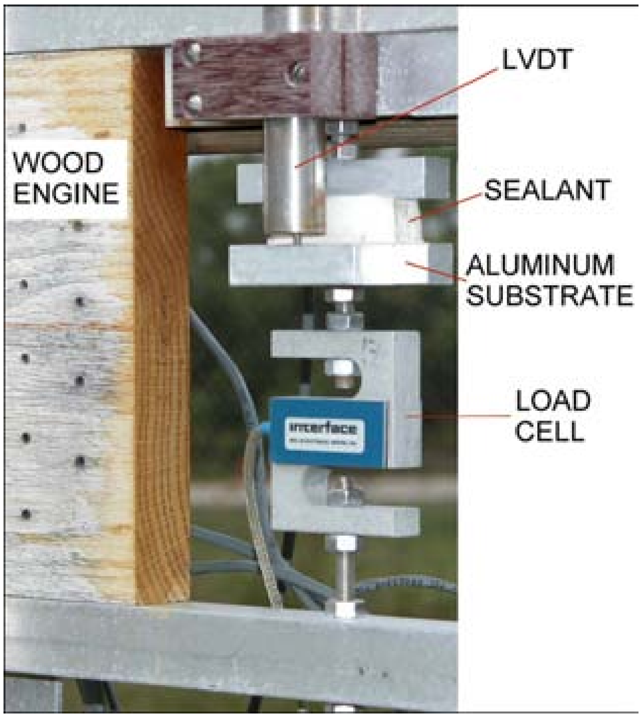

Figure 3. Detailed view of specimen mount.

Figure 4. The CFTA type outdoor exposure apparatus.

The entire apparatus may be tilted upward as much as 90° to maximize exposure to sunlight. Figure 4 shows 10 specimens mounted in the apparatus.

Each CFTA had 1.8-m-long beams to accommodate 20 specimens as well as actuators and positioning instrumentation. To ensure consistent strain across the CFTA, the upper and lower beams had to be stiff enough to minimize deflection under load. Standard aluminum I-beams were selected such that deflection would be less than 0.64 mm or 5% strain at maximum load, which would occur only beyond the designed test limit of 25% strain and only with relatively stiff specimens.

To ensure smooth linear motion, the lower beam was designed with wheels that run in tracks secured to the upper beam. This constrained the lower beam to move parallel to the upper beam. The design of the test apparatus was more fully described by Lacher *et al.* (2004).

Data Acquisition

Data collection and storage equipment was described previously (Williams *et al.* 2002).

Sealants

Seven different experimental sealants were formulated. The formulations were designed to have a range of properties and durability because the intent of this research is to establish a protocol for future work. Therefore, the sealants were selected to give different load deflection characteristics and have short service lives.

Methods

Data from the specimens were analyzed using a numerical mathematics package. Specimen response was measured for approximately 18 months.

A standard stress response test was developed to run on the CFTA. The test profile consists of moving the apparatus to the 0 position (no stress or strain on the specimens), waiting 2 min, ramping the strain to 10%, holding for 1 min, ramping the strain down to -10%, holding for 1 min, ramping the strain back to 0, and holding for 1 min. All movements were made at a constant rate of 20 mm/min.

Results and Discussion

The first challenge for an SLP test protocol is to establish a meaningful link between the degradation observed in the laboratory and that from outdoor exposure. The dose of some degrading factor in the laboratory and the dose of this factor outdoors also need to be linked. For example, if UV radiation is a key cause of degradation, the dose of radiation the specimens receive in the laboratory and outdoors must be measured. In the work described here, relevant weather parameters were measured and integrated with time to determine the dose that the specimens received. (For example, we know the total dose of UV radiation at the 18 different wavelengths.)
The second challenge of the test protocol is to find the appropriate material response to the dose. Load−deflection data (cyclic response) of the sealant were collected as the material weathered. These data enabled us to monitor changes in the stiffness of the sealant, detect adhesive and cohesive failures, and calculate the cumulative strain energy of specimens as they weathered. In an extended test, this information could be used to

determine the exact conditions leading to the failure of the test specimen.

Data Analysis

Figures 5 and 6 show the stress and strain for all specimens during 18 months for the TS apparatus. Figures 7 and 8 show stress and strain for all specimens during 16 months for the CS apparatus. The TS and CS apparatus were designed to give maximum–minimum strains of ±25%. However, these limits were exceeded several times during the exposure. The wood engine driving the cyclic movement gave almost the same strain on the different types of sealants (Figs. 6 and 8). The differences in the sealant formulations caused wide variation in the stress, which showed when all specimens were plotted (Figs. 5 and 7). The daily cyclic changes indicate the movement caused by changes in RH and temperature. The stress–strain response for individual specimens can be isolated from the data set for any specimen for any period of time during the exposure. For example, Figure 9 shows the stress–strain for three specimens during a 5-day period. The specimens show a hysteresis as they go through diurnal cycles. Specimens also may undergo smaller cycles during a day (Fig. 10). These smaller cycles are caused by the complex interaction of the thermal response of the sealant and the moisture-induced response of the wood engine. It occurs primarily with the softer sealant formulations. As of November 2003, some specimens had been exposed for more than a year and sufficient data were available to begin our analysis, which turned out to be far more complex than we had imagined when we began the experiment. Many of the experimental parameters did not fit our preconceived ideas. The data were analyzed in the following ways:

1. Daily cycles
2. Seasonal variations
    - Temperature
    - Relative humidity
    - Maximum–minimum stress
    - Maximum–minimum strain
3. Tests for significance
4. Elastic modulus

Daily cycles

In a typical laboratory fatigue test, a mean stress, amplitude, and frequency are prescribed and the material is cycled to failure. In outdoor tests, the cycles are not characterized that easily. We expected to observe diurnal cycles superimposed on a seasonal cycle. We did observe diurnal cycles, as shown in Figure 9. Several consecutive days are shown, but the cycles were quite different each day. In this case, the daily change in moisture content was superimposed on drying over several days.

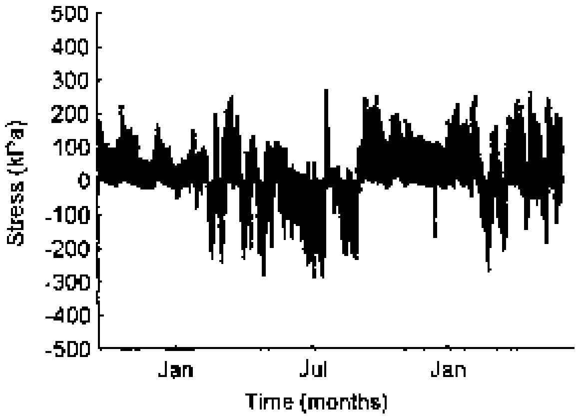

Figure 5. Stress versus time on CS type apparatus for an 18-month exposure period.

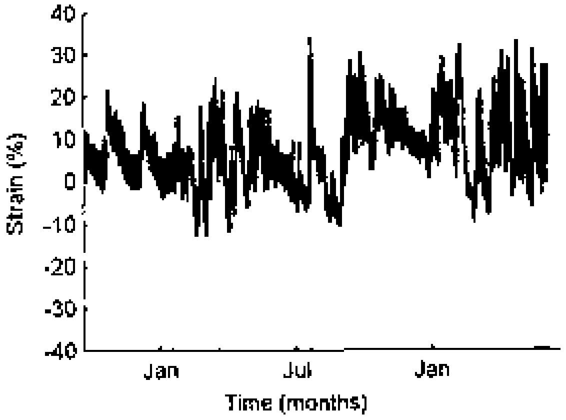

Figure 6. Strain versus time on CS type apparatus for an 18-month exposure period.

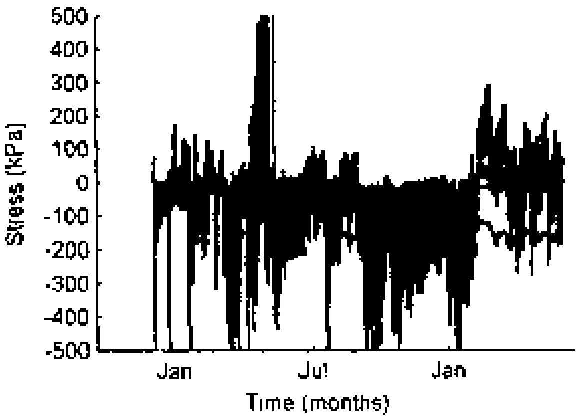

Figure 7. Stress versus time on TS type apparatus for an 18-month exposure period.

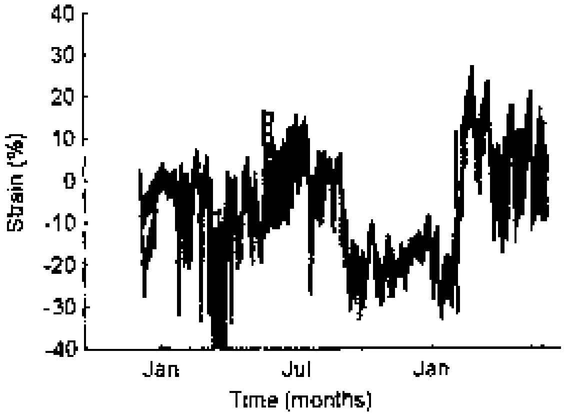

Figure 8. Strain versus time on TS type apparatus for an 18-month exposure period.

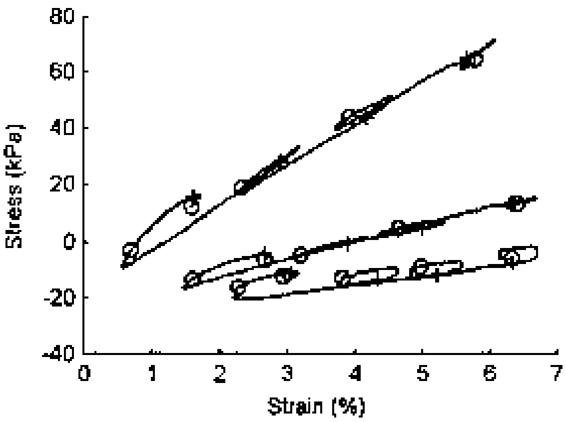

Figure 9. Stress versus strain plot highlighting temperature-induced looping phenomenon. Three different sealant formulations are shown.

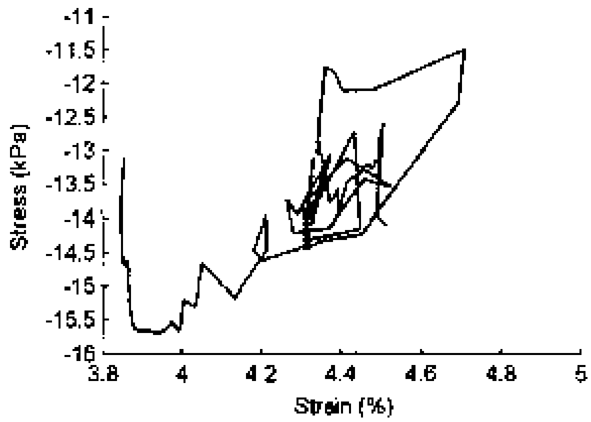

Figure 10. Stress versus strain plot for one day of complex movement.

The specimens were subjected to a cycle, but at a decreasing load and deflection on each of these days. When the wood became wetter over several days, it continually expanded and induced increased load-deflection with each daily cycle. In many cases, the cycle was further complicated by the lack of a clear diurnal cycle (Fig. 10). Several mini-cycles or loops occurred on the day shown in Figure 10. We suspect that this was caused by temperature-induced stress on days with intermittent cloud cover.

We also want to be able to quantify the frequency and magnitude of cyclic motion experienced by each specimen. However, defining a cycle as the unit of motion was problematic. During a single interval, we observed multiple changes in the strain direction that created strain loops of various sizes. Therefore, the number of cycles depended on the resolution of the analysis. We have calculated the number of cycles for different minimum loop sizes, and as expected, the number of calculated cycles decreased with increasing minimum loop size. We are currently working to develop a cumulative damage method based on cumulative stress or strain. The method involves analyzing the data in terms of accumulated stress−strain or accumulated stress−strain above some strain limit. This should take into account the different loops at different strains.

Seasonal variations

The yearly fluctuation in temperature, RH, and UV radiation measured at the outdoor exposure site near Madison, Wisconsin, is shown in Figures 11 through 13. Figure 11 shows the weekly maximum, minimum, and running 7-day mean temperatures experienced during the exposure. A similar plot for RH is shown in Figure 12. It is interesting that RH always reached 100% at least once each week, probably during the night when the temperature was at the dew point. The gaps in Figures 11 and 12 were caused by a computer failure. A back-up computer is now in place. Figure 13 is a similar plot for UV radiation intensity. The UV irradiance for 18 months is shown. The peak height shows the total irradiance at 323.45 nm for each week.

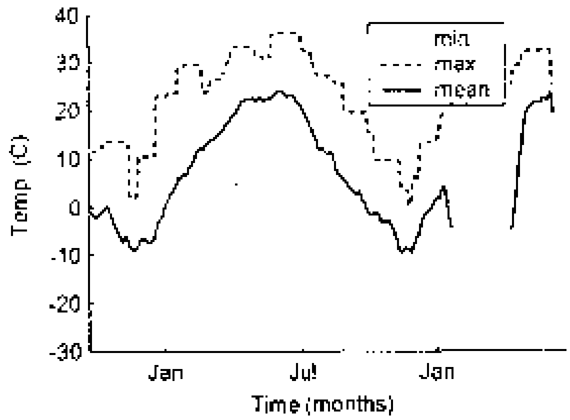

Figure 11. Yearly histogram of temperature. Maximum, minimum, and mean values are shown for week-long intervals.

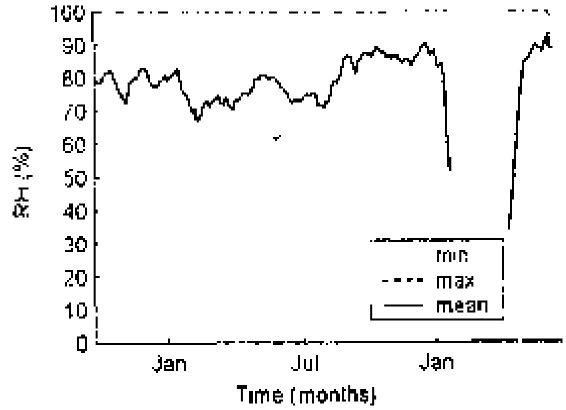

Figure 12. Yearly histogram of relative humidity (RH). Maximum, minimum, and mean values are shown for week-long intervals.

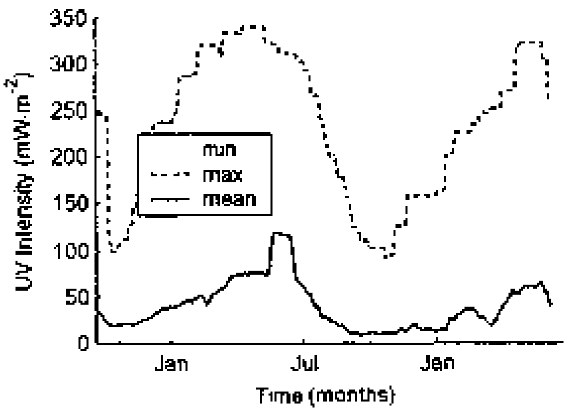

Figure 13. Yearly histogram of UV irradiance at 323.45 nm. Maximum, minimum, and mean values are shown for week-long intervals.

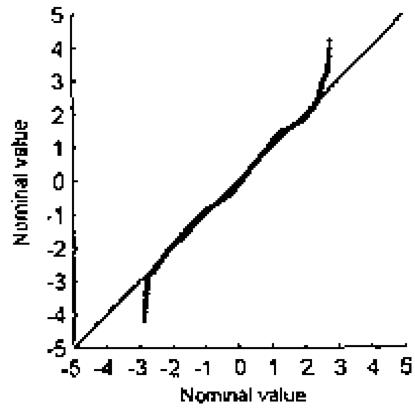

Figure 14. Normal value plot analysis showing statistical significance of data.

Tests for significance

Before beginning an exhaustive analysis of our data, we decided to apply some statistical tests to ensure that the data were nonrandom. For this purpose, we used a statistical tool called a normal value plot (NVP) (DeVor *et al.* 1992). An NVP measures data against a normal random distribution that has been scaled to match the extremes of the data. The straight-line portion of the NVP indicates variations in the data that are statistically random. The ends of the NVP that deviate from a straight line indicate nonrandom (deterministic cause and effect) variations in the data. Fortunately, our data were found to contain statistically significant variation. Figure 14 shows an NVP for the strain data from one specimen. We added a line at 45° for reference. From this figure, we can gather that the strain on this specimen is statistically significant -

meaning that it is caused by an underlying deterministic physical process rather than random noise. We made similar plots for all our data, and all plots show the data to be significant.

Elastic modulus

Our goal is to develop a cumulative damage model that will allow us to predict when sealants will fail. To do this, we need a measure of dose and a measure of performance. We developed dose measurements from the weather data. However, measurement of sealant performance is difficult. Our initial analysis involved using the load–deflection data to calculate the elastic modulus. We decided to use the elastic modulus as one measure of performance. As already discussed, changes in this property can be an early indicator of failure. We recognize that these are viscoelastic materials and do not give a true elastic modulus. However, we can obtain information on the degradation using this method. As mentioned previously, we are developing methods based on cumulative stress and strain, but have not completed our analysis as yet.

Initial stress and strain rates play a role in the measurement of elastic modulus. However, their role seems to be smaller by some orders of magnitude than the role of temperature. We have the ability to Select one exposure temperature and still have enough data to work with. Therefore, we selected all data collected at a constant temperature, in this case 20°C. We could have selected data at any temperature for which we had data (-20°C to +20°C). To obtain the elastic modulus, we can construct piecewise linear fits of the data.

We must consider two things in fitting the data. First, we must determine how many points to fit (that is, the width of the window). Second, we must determine how tight a fit is required before we trust that it is an accurate model of what is really happening. Figure 15 shows the combined effect of these two analyses for all data from one specimen taken at 20°C. At a window width of 3 and R^2 of 90%, there are about 7000 segments, whereas for a window of 10 and R^2 of 99.99% tolerance, there are almost no segments. If one chooses a width of 5 points and R^2 = 99%, about half the data remain in the data set. In this analysis, there is no attempt to choose a type of cycle. Wider windows or tighter fits do obtain fewer outlying points, but they also discard a large number of points that we consider acceptable.

Figure 16 show the segments (modulus) for one specimen for 18 months. There is considerable spread in the data. This is caused by the segments being taken at different initial strains and different strain rates, both of which can affect the elastic modulus. The gaps in the data occurred during the winter–spring when the temperature seldom reached 20°C. For this specimen, there was no apparent change in modulus. If there was a change in modulus, a similar data treatment can show this (Fig. 17). This specimen shows considerable decrease in elastic modulus during the 18 months.

The change in modulus can also be determined by plotting stress–strain across selected periods at different times (Fig. 18). Figure 18 shows the stress–strain plot for

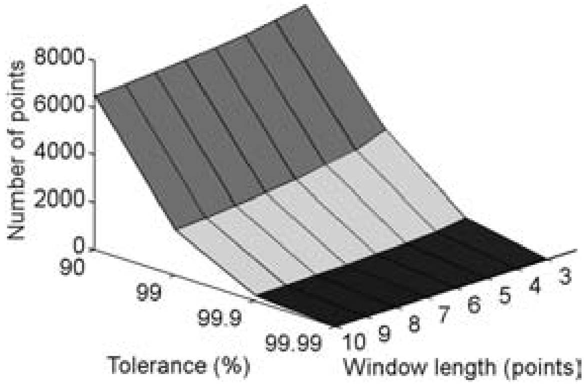

Figure 15. Analysis of data breakdown procedure. When selecting a fit to given R^2 tolerance (on the *x* axis), using a given window length (on the *y* axis), the *z* axis gives the number of points obtained.

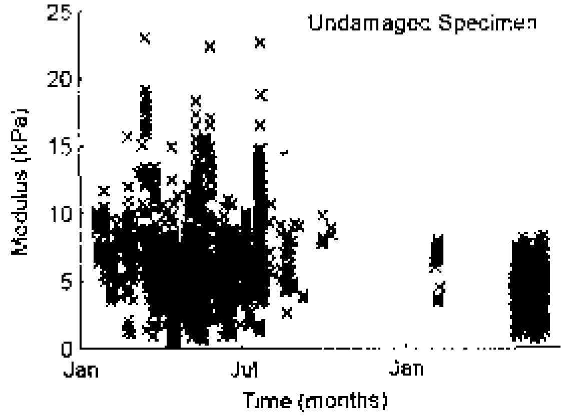

Figure 16. Apporximated elastic modulus (suing the R^2 > 99%, *w* = 4 fitting method) for an undamaged specimen.

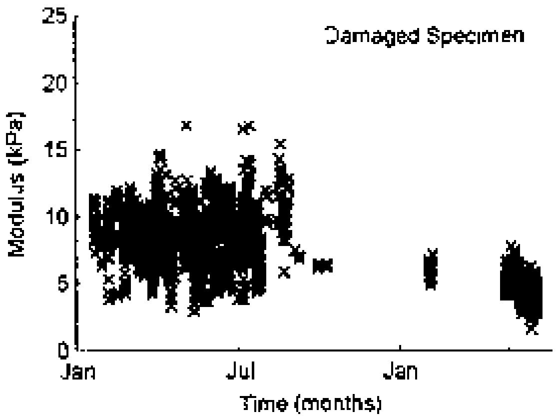

Figure 17. Approximated elastic modulus (using the R^2 >99%, *w* = 4 fitting method) for a damaged specimen.

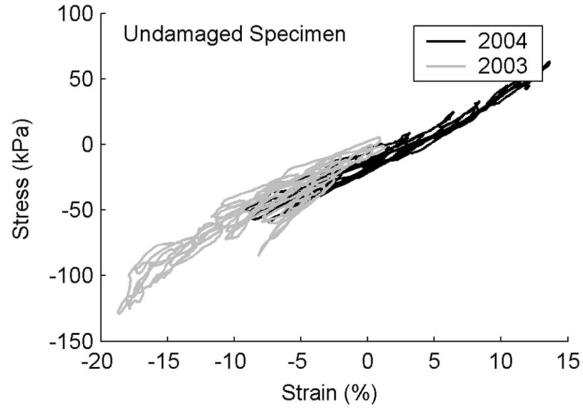

Figure 18. Comparison of stress and strain behavior of an undamaged specimen for three-moth periods in 2003 and 2004.

the same specimen as shown in Figure 16. The stress–strain plots are for April–June of 2003 and 2004; this specimen shows no change in modulus. The plots from both years have the same slope. Figure 19 shows the stress–strain plot for the specimen evaluated in Figure 17. There was considerable change in the slope between the two years. The decreased slope (apparent modulus of elasticity) is caused by the opening of voids in the sealant and debonding from the substrate that resulted in a decrease in the effective cross-sectional area of the specimen. Similar undamaged specimens showed an increase in apparent modulus during the same period.

By analyzing the data during the year, it is possible to determine whether the change was gradual as might occur if the specimen degraded by polymer chain cleavage or

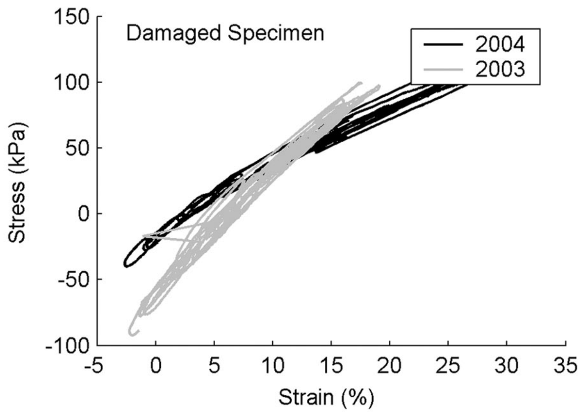

Figure 19. Comparison of stress and strain behavior of a damaged specimen for three-month periods in 2003 and 2004.

abrupt as might occur if the specimen failed in adhesion or cohesion. Data analysis revealed that this specimen failed abruptly and inspection of the specimen confirmed this (Fig. 20). The specimen failed both cohesively and adhesively. Review of the data can also reveal the time and conditions at which the failure occurred (Fig. 21). Figure 21 shows several cycles with an abrupt change in the slope of the stress–strain plot. This abrupt change occurred at 2:27 p.m. on May 12,2004, following a day of rain.

We are continuing our investigations and exploring other methods for evaluating the data, such as cycles to failure, accumulated stress to failure, and accumulated strain to failure. These analyses would be improved by having stress response data from controlled strain experiments at various times during the exposure. This is not possible with apparatus in which the drivers are linked directly with the specimens. Dimensional change of the engines was directly transferred to the specimens. This makes it difficult to perform designed experiments that require some stressors to be turned off for some specimens. Unfortunately, engines that are either thermal- or moisture-driven (primarily wood and plastic) are subject to variability between engines because no two wood blocks or plastic tubes are exactly the same. Wood and plastic engines also tend to change as they age. This makes exact replication of experiments virtually impossible, not only between test apparatuses but within the same apparatus when multiple engines are used. Another disadvantage of this type of test apparatus is the difficulty of ensuring that the strain imposed on the specimens is of a specific amplitude about a prescribed mean value (zero in present experiments). Though the amplitude is determined by the size of the engines, material variability limits the precision with which the amplitude can be controlled. To center the strain about zero, specimens must be pre-strained at the time of installation to match the instantaneous state of the engines. Further, the mean dimensions of the engines change with seasonal variations in weather. Physical adjustment of the specimens is required to correct asymmetric strain.

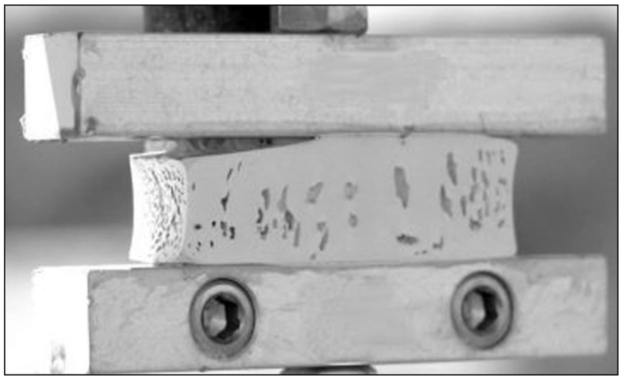

Figure 20. Close-up view of a damaged specimen.

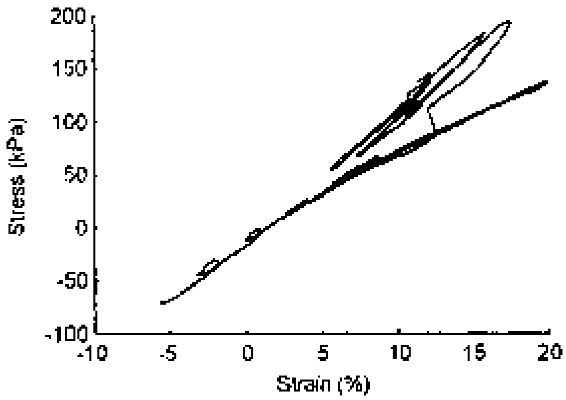

Figure 21. Sudden failure of a specimen. The change in slope occurred on May 12, 2004, at 14:27 CST. Ambient temperature was 19°C. Ambient RH was 45%. It had rained the previous day. The wood engine in the CS apparatus was in a drying cycle, which placed tension on the specimen.

Computer-Controlled Powered Cyclic Fatigue Test Apparatus

In July–August2003, we designed and built a new CFTA that could be computer controlled. This would require using precisely controllable linear actuators in place of wood, plastic, or metal engines, designing new hardware and electronic controls, and developing control software. The advantages offered by a computer-controlled CFTA are consistency from one test to another and almost uniform strain among specimens on the same apparatus. The strain uniformity is limited only by the physical compliance of the CFTA, which can be minimized with proper design.

In previous testing using the TS and CS apparatus, measured sealant material properties varied greatly with strain rate and initial stress. Therefore, differences in sealant modulus of elasticity caused by material degradation were confounded with differences caused by test conditions. The standard stress response test uses computer control of the CFTA to impose a precise strain profile on multiple specimens simultaneously and records the resultant axial forces on each specimen. The standard stress response test always begins at zero strain and has a constant strain rate. Therefore, the data allows calculation of specimen material properties that can be directly compared both between specimens within a single test to detect differences between sealant formulations and specimen to specimen variation within a formulation and between repeated standard stress response tests to detect changes caused by outdoor exposure. By repeating the standard stress response test at different ambient temperatures, we hope to develop a temperature correction for measured modulus of elasticity that can be applied to existing stress–straindata from wood engine data.

A computer-controlled CFTA offers a great deal of experimental flexibility. It can be programmed to receive input from the thermal response of a metal or plastic or a moisture response from wood. The CFTA can be programmed to produce strain in the same or the opposite direction of thermal- or moisture-driven expansion or contraction, and a gain factor may be set with software. The CFTA also can be commanded to move in an arbitrary manner determined by the programmer. This allows a specific strain history to be repeated at other times or replicated by another CFTA at a different location, such as in a controlled laboratory environment. This also enables the computer-controlled CFTA to execute a specific strain versus time profile at a particular time or when environmental conditions are within specified limits. This can serve as an *in situ* experiment that measures a material property of the specimen that is associated with the amount of damage sustained by the specimen. Such periodic testing will be used to acquire data needed to determine dose damage relationships.

Thermal- and moisture-driven apparatuses must be designed conservatively with relatively small wood engines to avoid specimen strains exceeding ±25%. The computer controlled CFTA uses software to limit strain to a preset value (for example, ±25%) during extreme conditions. Therefore, the CFTA moves more aggressively than reactive engine testers during normal weather conditions. Computer-controlled CFTAs compensate for asymmetric strain profiles with programmable zero offsets. Current wood engine apparatus require physical adjustment of the specimens to correct this problem.

With the CFTA, standard stress response experiments were done on five of the formulations at the time of installation in the CFTA. Figure 22 shows the strain profile imposed on the specimens. The stress responses are shown for two specimens with different formulations (Figs. 23 and 24). The two formulations responded quite differently to the test, both in the magnitude of the resultant stress (a function of modulus of elasticity) and the amount of stress relaxation during the constant strain holding periods. Stress versus strain plots for the two formulations show differences in modulus of elasticity (slope) and the amount of stress relaxation (length of vertical lines) (Figs. 25 and 26). The responses shown in Figures 25 and 26 are for sealant

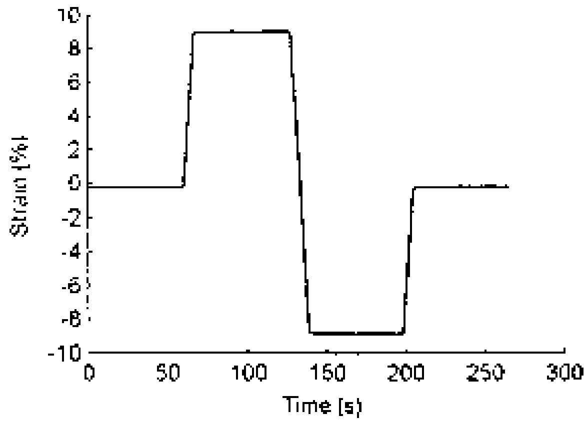

Figure 22. Strain profile for a standard stress response test.

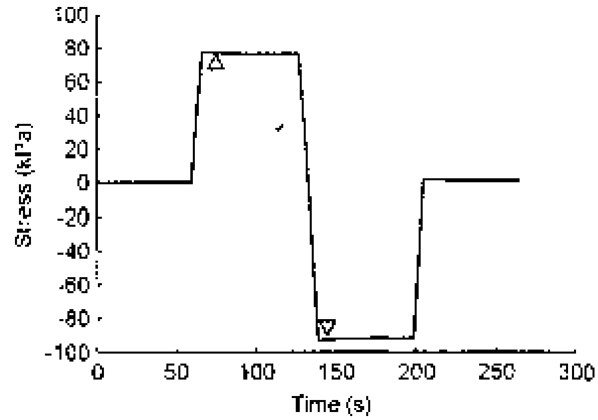

Figure 23. Stress profile obtained from an standard stress response test for a stiff specimen. Note the slight relaxation indicated by the arrows.

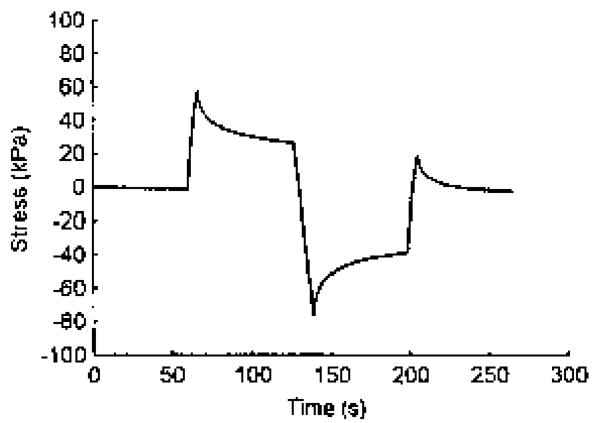

Figure 24. Stress profile obtained from standard stress response test for a soft specimen. The relaxation is much more pronounced than shown in Figure 23.

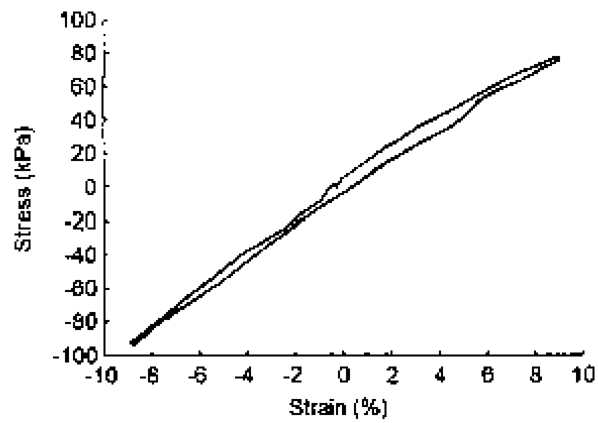

Figure 25. Stress and strain profile for the stiff specimen from Figure 23.

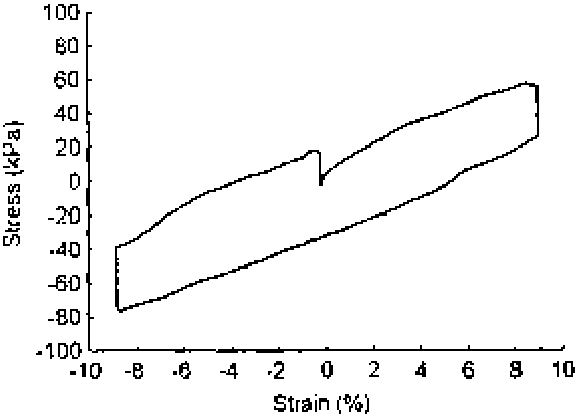

Figure 26. Stress and strain profile for the soft specimen from Figure 24.

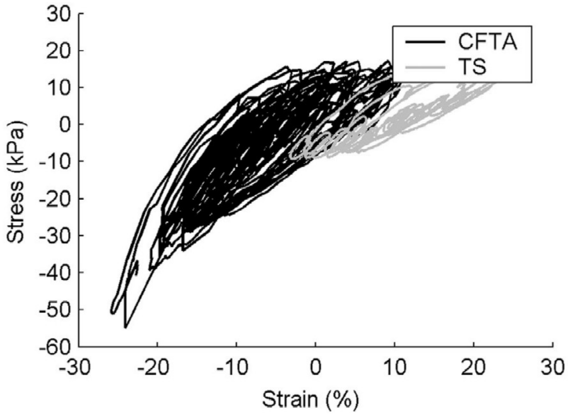

Figure 27. Comparison of stress and strain profiles for replicates of a soft formulation on the TS type apparatus and the CFTA type apparatus.

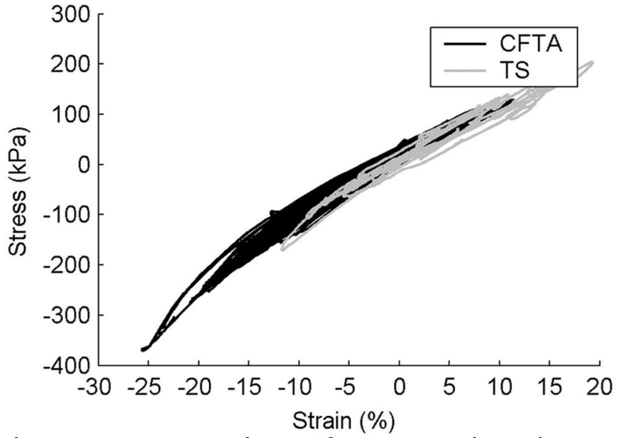

Figure 28. Comparison of stress and strain profiles for replicates of a stiff formulation on the TS type apparatus and the CFTA type apparatus.

formulations with low and high flexibility, respectively. These initial characterizations of the specimens will be compared with standard stress response tests conducted periodically during outdoor exposure. It is expected that specimen degradation and/or changes in material properties will be evidenced by differences in stress response plots.

In the present configuration of the CFTA, the cyclic fatigue is generated by thermally driven changes in black aluminum. This gives more rapid cycling than the wood-driven apparatus. However, the data from the CFTA are comparable with the data from the wood-driven apparatus (Figs. 27 and 28). The stress–strain plots for the two formulations are almost the same for the two types of apparatus.

Conclusions

We have demonstrated that the response of sealants and the weather causing the response can be monitored continuously. For the outdoor exposure of the sealants used in this work, weather-induced cyclic fatigue of specimens and the documentation of stress and strain during this cyclic movement were deemed to be critical aspects of the experiment. The data can be analyzed to determine the elastic modulus of the material. A decrease in the load on the specimen could indicate polymer deterioration, loss of adhesion to the substrate, or cohesive failure of the sealant. The occurrence of these types of changes can be linked to the weather causing the degradation, and changes can be evaluated in terms of weather dose, not time of exposure. A new type of test apparatus has been built to allow *in situ* standard stress response experiments during outdoor exposure. The development of the wood-driven test apparatus gave us the capability to track sealant response to the weather on a minute-by-minute basis, but this apparatus lacked the capability to do *in situ* tests. The development of the computer-controlled apparatus makes it possible to input fatigue cycles from a variety of weather-generated inputs (moisture movement of wood, thermal movement of metals, complex movements from actual structures) or from a computer-generated cycle.

Acknowledgments

We thank Russell Goodrich and Patrick Neale (Smithsonian Environmental Research Center) for their help in setting up, calibrating, and monitoring the UV radiometer; Dave Eustice and Larry Zehner (FPL) for building the test apparatus; and all the members of the FPL shops for their help with the initial stages of setting up the experiment.

References

ASTM. 2000. *Annual Book of ASTM Standards,* Vol. 04.07, American Society for Testing and Materials, Philadelphia, PA.

C 718 93, Standard test method for ultraviolet (UV)-cold box exposure of one-part, elastomeric, solvent-release type sealants.

C 719 98, Standard test method for adhesion and cohesion of elastomeric joint sealants under cyclic movement (Hockman cycle).

C 732 95, Standard test method for aging effects of artificial weathering on latex sealants.

C 734 93, Standard test method for low-temperature flexibility of latex sealants after artificial weathering.

C 793 97, Standard test method for effects of accelerated weathering on elastomeric joint sealants.

C 1257 94, Standard test method for accelerated weathering of solvent-release-type sealants.

C 1442 99, Standard practice for conducting tests on sealants using artificial weathering apparatus.

D 2249 94, Standard test method for predicting effect of weathering on face glazing and bedding compounds on metal sash.

ASTM. 2001. *Annual Book of ASTM Standards,* Vol. 06.01, American Society for Testing and Materials, Philadelphia, PA.

D 822 96, Standard practice of conducting tests on paint and related coatings and materials using filtered open-flame carbon-arc light and water exposure apparatus.

D 4587 91, Standard practice of conducting tests on paint and related coatings and materials using a fluorescent UV-condensation light- and water-exposure apparatus.

D 5031 96, Standard practice of conducting tests on paint and related coatings and materials using enclosed carbon-arc light and water exposure apparatus.

G 26 96, Standard practice for operating light-exposure apparatus (xenon-arc) with and without water for exposure of nonmetallic materials.

G 53 96, Standard practice for operating light- and water-exposure apparatus (fluorescent UV-condensing type) for exposure of nonmetallic materials.

Brown, N. G. 1965. Assessment of joint sealant by outdoor exposure in cyclic movement testers. Report No. 01.1 .-2, CSIRO Division of Building Research, Highett, Victoria, Australia, p. 16–22.

Burstrom, P. G. 1980. Durability and a in of sealants. In: *Durability of Building Materials and Components,* ASTM STP 691, P. J. Sereda and G. G. Litvan, eds., ASTM, Philadelphia, PA, USA, p. 643–657.

DeVor, R. E., Chang, T.–H.,and Sutherland, J. W. 1992. *Statistical Qualify Design and Control,* Prentice Hall, Upper Saddle River, NY, p. 90–94.

Hunston, D. L., White, C. C., Williams, R. S. 2003a. Mechanical Behavior of Caulks and Sealants. Proceedings of the 225th ACS National Meeting, New Orleans, LA (Inpress).

Hunston, D. L., White, C. C., Williams, R. S. 2003b. Viscoelastic Characterization of Sealant Materials. In: Proceeding of the 26th Annual Meeting of the Adhesion Society, Myrtle Beach, SC (In press).

Karpati, K. K., Solvason, M. R., and Sereda, P. J. 1977. Weathering rack for sealants. *Journal of Coatings Technology* 49(626): 44-47.

Lacasse, M. A. 1994. Advances in test methods to assess the long term performance of sealants. In: *Science and Technology of Building Seals, Seals, Sealants, Glazing and Waterproofing,* J. C. Myers, ed., Vol. Ill, ASTM STOP 1254, American Society for Testing and Materials, Philadelphia, PA. p. 5–20.

Lacher, L., Williams, R. S., and Halpin, C. 2004. Development of a powered outdoor sealant fatigue test apparatus. In: Proceedings: Third International Symposium on Service Life Prediction, Feb 1–6,2004. Sedona AZ (In press).

Martin, J. W. 2000. A critical review of the role of field-exposure experiments in predictin the service life of coatings. In: *Plastics and Coatings Durability, Stabilization, Testing,* R. A. Ryntz, ed., Ch. 2, Hanser Gardner Publications, Inc., Cincinnati, OH. p. 32

Onuoha, U. 0. 1999. Durability of one-part polyurethane and polyurethane hybrid sealants. In: *Durability of Building Sealants,* A. T. Wolf, ed., RILEM, France. p. 235–251.

White, C. C., Martin, J., Weber, S., Shultz, L., and Williams, R. S. 2002. Reliability-Based Method for Service Life Prediction of Materials. In: Proceeding from SPE/ANTEC National Meeting, May, 2002.

White, C. C., Hunston, D. L., and Williams, R. S. 2003. Challenges in Characterizing Sealant. In: Proceedings of the ANTEC conference from Society of Plastics Engineering, Nashville, TN.

White, C. C., Embree, N., Buch, C., and Williams, R. S. Design, 2004. Development and Testing of a Hybrid *in-situ* Testing Device for Sealant, Review of Scientific Instrumentation. (In Press).

Williams, R. S., Sanandi, A., Halpin, C., and White, C. 2002. Merging weather data with materials response data during outdoor exposure. Paper 17. In: Proceedings of the Third International Woodcoatings Congress, 28-30 October, The Hague, The Netherlands.

Williams, R. S., Lacher, L., Halpin, C., and White, C. 2004. Evaluating weather factors and material response during outdoor exposure to determine accelerated test protocols for predicting service life. In: Proceedings, Third International Symposium on Service Life Prediction, Feb 1-6, 2004, Sedona AZ. (In press).

Wolf, A. T. 1999. Attempts at correlating accelerated laboratory and natural outdoor ageing results. In: *Durability of Building Sealants,* A. T. Wolf, ed., RILEM, France, p. 181–201.

Fourth International Woodcoatings Congress

WOODCOATINGS

Developments for a Sustainable Future

25 - 27 October 2004 • The Netherlands Congress Centre • The Hague

PRA COATINGS TECHNOLOGY CENTRE

Congress Papers

4th International Woodcoatings Congress

Developments for a Sustainable Future

The Hague, The Netherlands

25 - 27 October 2004

CONGRESS PAPERS

Published by:

The Paint Research Association
8 Waldegrave Road, Teddington
Middlesex, TW11 8LD, UK

ISBN 0-9543164-9-5